

## Enhanced Photochromic Modulation Efficiency: A Novel Plasmon

### Molybdenum Oxide Hybrid

Ning Li<sup>a, c</sup>, Yamei Li<sup>b</sup>, Guangyao Sun<sup>a</sup>, Yijie Zhou<sup>a</sup>, Shidong Ji<sup>a</sup>, Heliang Yao<sup>a</sup>, Xun Cao<sup>a, \*</sup>,  
Shanhu Bao<sup>a, \*</sup>, Ping Jin<sup>a, \*</sup>

<sup>a</sup>State Key Laboratory of High Performance Ceramics and Superfine Microstructure, Shanghai  
institute of Ceramics, Chinese Academy of Sciences, Dingxi 1295, Changning, Shanghai, 200050,  
China

<sup>b</sup>Biofunctional Catalyst Research Team, Riken, 2-1 Hirosawa, Wako, Saitama 351-0198, Japan

<sup>c</sup>University of Chinese Academy of Sciences, Beijing 100049, China

#### Experimental detail

The MoO<sub>3-x</sub> hybrid was also prepared by a simple hydrothermal method with sodium molybdate and oxalic acid. Sodium molybdate was added into the mixture of 50ml distilled water, and 10ml saturated oxalic acid, and then drop hydrochloric acid to PH=1 and then transfer the mixture into the Teflon-line stainless steel autoclave for hydrothermal treatment at 120°C, 48h. After reaction, the white suspension was allowed to cool naturally to room temperature, following which the products were filtered and washed several times with deionized water, and then dried in ambient air at 50 °C for 4 h.

The crystal phase of the as-prepared powders were determined by x-ray diffraction (XRD) with Cu-K $\alpha$  radiation (1.541 Å, 40 mA, 40 kV) at a scanning rate of 5°/min over a 2 $\theta$  range from 10° to 90°. The microscopic powder morphology was obtained by using a field-emission scanning electron microscope (FE-SEM, HITACHIS-3400, Japan) at an acceleration voltage of 15 kV. The powder composition and microstructure were investigated by TEM (JEOL2010) with an energydispersive spectrometer (EDS) attachment (HITACHIH-800, Japan). Selected-area electron diffraction (SAED) was also used to characterize the powder.

The optical properties were characterized by applying UV–visible spectrometry (HITACHI U-3010) over 350–2600 nm to films made by mixing the nanopowder and resin under the same

concentration and then blade coating the composite onto the substrates. The scanning speed was 600 nm/min. “Virgin” samples refer to samples before irradiation, whereas “colored” samples refer to samples in the colored state (i.e., after 300 W UV irradiation for ~5 min by a xenon lamp).

The photoluminescence spectrum was tested by the fluorescent spectrometer Lumina (Thermo Fisher Scientific) and the valence state and elemental composition of the MT powder were analyzed by x-ray photoelectron spectrometry (XPS, XPS ESCALAB 250, Thermo Fisher Scientific) with irradiation at the Al K $\alpha$  line. The pass energy and step size were 20.0 eV and 0.05 eV, respectively. All XPS spectra were calibrated by using the C 1s peak at 284.8 eV.

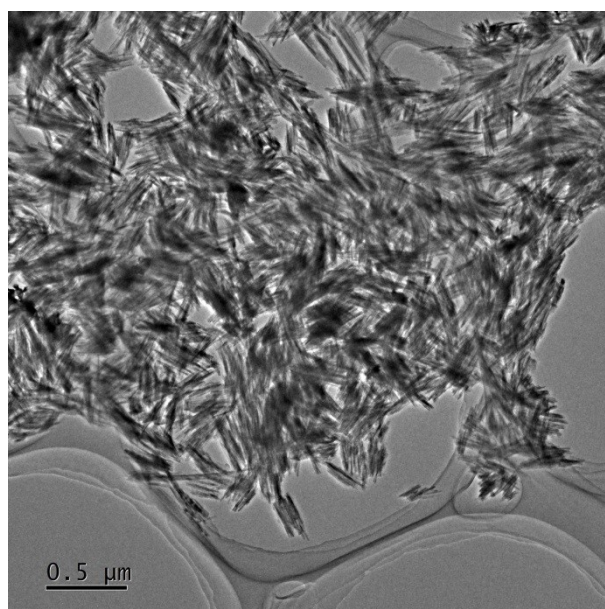


Figure s1: the TEM image of the MoO<sub>3-x</sub> Hybrid.

Figure s1 show the morphology of the the MoO<sub>3-x</sub> Hybrid at a low magnification and the samples look like leaves stacked together.

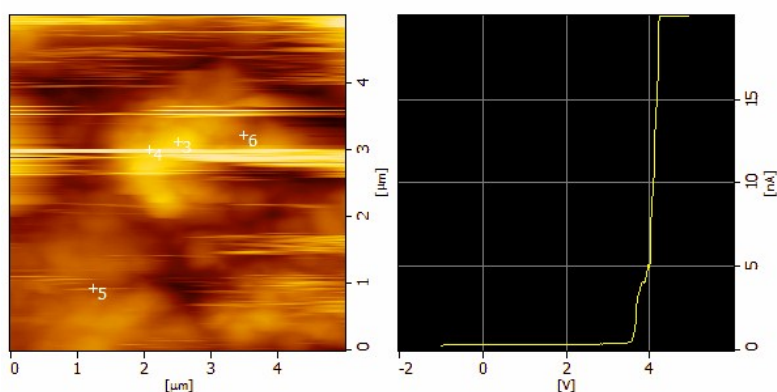


Figure s2 Electric properties of the MoO<sub>3-x</sub> hybrid by C-AFM

The prepared nanopowder press as piece and test IV curve by AFM. The nanopowder has good electrical conductivity.

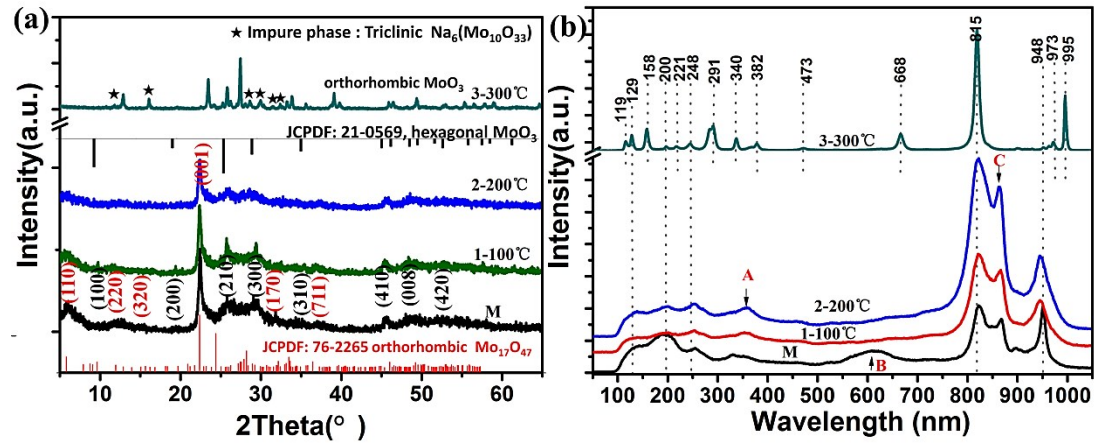


Figure s3: XRD (a) and Raman spectrum (b) of the  $\text{MoO}_{3-x}$  hybrid (named M) and a series of samples with different annealed temperature.

As shown in Figure s3, the sample with different annealed temperature gradually transfer  $\text{Mo}_{17}\text{O}_{47}$  to  $\text{MoO}_3$  due to the peak intensity of  $\text{Mo}_{17}\text{O}_{47}$  decreasing, especially at  $2\theta=22.485$ . After annealing at  $300^\circ\text{C}$ , the sample transfer to orthorhombic  $\text{MoO}_3$  (JCPDF: 76-1003) with a little impure phase of  $\text{Na}_6(\text{Mo}_{10}\text{O}_{33})$  (JCPDF: 76-2189), due to Na doped. For the Raman analysis in Figure s3(b), the peak positions are indexed at 995 ( $A_g$ ,  $\nu_{\text{as}}$  M=O stretch), 668 ( $B_{2g}$ ,  $B_{3g}$ ,  $\nu_{\text{as}}$  O-M-O stretch), 473 ( $A_g$ ,  $\nu_{\text{as}}$  O-M-O stretch and bend), 382 ( $B_{1g}$ ,  $\delta$  O-M-O scissor), 340 ( $A_g$ ,  $B_{1g}$ ,  $\delta$  O-M-O bend), 291 ( $B_{3g}$ ,  $\delta$  O=M=O wagging), 248 ( $B_{3g}$ ,  $\tau$  O=Mo=O twist), 221 ( $A_g$ , rotational rigid  $\text{MoO}_4$  chain mode,  $R_c$ ), 200 ( $B_{2g}$ ,  $\tau$  O=Mo=O twist), 158 ( $A_g/B_{1g}$ , translational rigid  $\text{MoO}_4$  chain mode,  $T_b$ ), 129 ( $B_{3g}$ , translational rigid  $\text{MoO}_4$  chain mode,  $T_c$ ), 119 ( $B_{2g}$ , translational rigid  $\text{MoO}_4$  chain mode,  $T_c$ )<sup>1,2</sup>. Before annealing, the sample has weak peak intensity at 100-400nm, and many peaks coincide such as A. A swell at 600nm (B) and the broad peaks at 800-1000nm are ascribed to amorphous state. After annealing, the swell disappeared, demonstrating amorphous state transferring to crystalline state. Meanwhile, the Raman peaks at 800-1000 nm increased with the annealed temperature, and those peaks at 100-400 nm decreased, demonstrating Mo=O get better intensity and increase but Mo-O decreases which imply the oxygen deficiency decrease and the hybrid changes to  $\text{MoO}_3$ .

$$E(\lambda) = \frac{24\pi^2 N a^3 \epsilon_m^{3/2}}{\lambda \ln(10)} \left[ \frac{\epsilon_i}{(\epsilon_r + \chi \epsilon_m)^2 + \epsilon_i^2} \right]$$

The Mie theory is

$E(\lambda)$  = Extinction spectrum = absorption + scattering,  $a$  is related to the size (the diameter of

sphere),  $\chi$  is the shape factor (2 for sphere,  $>2$  for spheroid) related to the morphology<sup>3</sup>

According to the Mie theory, the size increase, the absorption peak shift to long wavelength range.

For nanorod, according to Gans theory, the size is expressed by aspect ratio  $R=A/B$  (A is the length, B is the diameter). The nanorod has two extinction Modes: Transverse Mode in visible region and Longitudinal Mode in Near-infrared region. When the aspect ratio decreases, the longitudinal Mode shifts to short wavelength range.

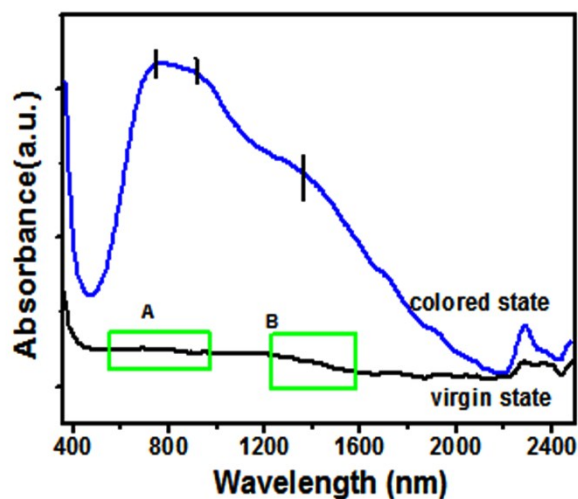


Figure S4 the absorption spectra of the  $\text{MoO}_{3-x}$  hybrid in virgin state and colored state.

1. M. Dieterle, G. Weinberg, G. Mestl. *Phys Chem Chem Phys* **2002**, 4, (5), 812-821.
2. J. V. Silveira, J. A. Batista, G. D. Saraiva, J. Mendes Filho, A. G. Souza Filho, S. Hu, X. Wang. *Vibrational Spectroscopy* **2010**, 54, (2), 179-183.
3. K. Manthiram, A. P. Alivisatos. *J Am Chem Soc* **2012**, 134, (9), 3995-8.